Review Article

Microbiology & Infectious Diseases

Design of Improved Anti-Influenza Peptide Mimetics Using In Silico Molecular Modeling

Kenneth A. Mwawasi[1], David C. Bulir[3], Seiji N. Sugiman-Manrangos[4], Murray S. Junop[6], Christopher Stone[3,5], and James B. Mahony[2,3,5*]

[1]*McMaster Immunology Research Center, Canada.*

[2]*M.G. DeGroote Institute for Infectious Disease Research, Canada.*

[3]*The St. Joseph's Research Institute, St. Joseph's Healthcare Hamilton, Ontario, Canada.*

[4]*Department of Biochemistry and Biomedical Sciences, McMaster University, Hamilton, Ontario, Canada.*

[5]*Department of Pathology and Molecular Medicine, McMaster University, Hamilton, Ontario, Canada.*

[6]*Department of Biochemistry, Schulich School of Medicine & Dentistry, Western University, London, Ontario, Canada.*

***Correspondence:**
Mahony JB, Regional Virology Laboratory, St. Joseph's Healthcare Hamilton, 50 Charlton Ave. E, Hamilton, Ontario, Canada, Tel: (905) 522-1155; Ext: 35013; Fax: (905) 521-6083; E-mail: mahonyj@mcmaster.ca.

Received: 19 July 2017; **Accepted:** 05 August 2017

Citation: Kenneth A. Mwawasi, David C. Bulir, Seiji N. Sugiman-Manrangos, et al. Design of Improved Anti-Influenza Peptide Mimetics Using In Silico Molecular Modeling. Microbiol Infect Dis. 2017; 1(1): 1-8.

ABSTRACT

Influenza virus is a major respiratory virus infection responsible for seasonal outbreaks, global pandemics, and an estimated 500,000 deaths annually. The RNA polymerase of influenza virus is a heterotrimeric enzyme complex made up of three subunits that interact to form an active holoenzyme. In this study, in silico molecular modeling was used to predict the hypothetical free energy of binding between the PB1 and PA subunits for various single amino acid substitutions within the PB1 subunit. Two significant substitutions for threonine at position six were identified: glutamic acid (T6E) and arginine (T6R). We engineered native and modified PB1 peptide mimetics with a carrier protein and a cell penetrating peptide (HIV Tat NLS) to deliver the peptides to cells. These peptide mimetics inhibited Influenza a virus transcription and translation in MDCK cells in a dose-dependent manner with 98% inhibition at 50 μM. The inhibitory activity of peptide mimetics containing T6E and T6R substitutions, were three- to four-fold higher than the wild type peptide consistent with the in silico molecular modeling prediction. These results demonstrate that molecular modeling of protein-protein interactions can be used to design peptide mimetics as protein therapeutics which have increased anti-viral activity.

Keywords

Peptide mimetics, Influenza virus, Anti-viral activity.

Introduction

Influenza is a major infectious burden in humans causing seasonal outbreaks with tens of millions of infection every year and 250,000-500,000 deaths worldwide [1,2]. Influenza A is responsible for global pandemics with the 1918 pandemic causing an estimated 40 million deaths worldwide, and the most recent pandemic strain, 2009 pH1N1, spreading to over 175 countries worldwide in just a few months [3,4].

The main strategy for prevention and control of influenza over the past 60 years has been vaccination. While vaccines continue to be an effective strategy for controlling infection, influenza vaccines must be remanufactured every year since influenza is constantly mutating, making existing vaccines less effective against new emerging strains. Antivirals have been shown to be effective against Influenza and are especially important during an outbreak where vaccines may not provide protection against new strains. The two most routinely used classes of drugs for influenza treatment are the M2 ion channel inhibitors including amantadine and rimantadine, and the Neuraminidase inhibitors (NAIs), such as oseltamivir

and zanamivir [2]. However, in recent years these antiviral drugs have become less effective in treating influenza due to mutations conferring antiviral resistance. Since 2006, over 90% of circulating influenza strains has developed resistance to adamantanes due to a S13N mutation in the M2 protein [5]. Additionally, an H275Y mutation in the neuraminidase gene which confers resistance to oseltamivir has been observed in approximately 2% of Influenza strains tested [6]. Therefore, there is a growing need for new anti-Influenza therapeutics.

The influenza RNA-dependent RNA polymerase is a heterotrimeric complex consisting of three protein subunits that direct mRNA transcription and genomic replication. The PB1 protein is the catalytic component responsible for transcription and RNA replication, while the PB2 and PA subunits are involved in cap-snatching [7-9]. The heterotrimeric complex is formed by the interactions between the N-terminus of PB1 with the C-terminus of PA and the C-terminus of PB1 with the N-terminus of PB2. The central domain of PB1 is the catalytic RNA processing domain, and therefore PB1 is considered both the catalytic core and structural backbone of the viral polymerase. The high degree of amino acid sequence conservation within the polymerase subunits is consistent with the essential role of this enzyme and presents a novel target for drug development [10].

The interaction between the polymerase subunits has been studied using X-ray crystallography. Co-crystallization studies have shown that the N-terminus of PB1 ($PB1_{1-15}$) interacts with the C-terminus of PA ($PA_{257-716}$) via extensive hydrogen bonding and hydrophobic interactions, thereby providing a potential drug target [11,12]. Ghanem et al. showed that plasmids expressing a $PB1_{1-25}$ peptide when transfected into HEK293T cells reduced virus replication after infection with influenza virus [13]. We used *in silico* ZMM molecular modeling to analyze the PB1-PA interaction and developed novel peptide mimetics with increased antiviral activity. When these novel peptides are conjugated to a carrier protein containing the HIV Tat_{47-57} cell penetrating peptide for nuclear localization [14] they entered cells and inhibited virus replication at low micromolar concentrations. These peptide mimetics therefore represent a novel class of therapeutics which if efficacious in animal studies could provide an additional therapeutic to combat human influenza outbreaks.

Materials and Methods

PB1 protein ClustalW alignment

PB1 subunit sequences of 12 different Influenza A strains were examined to determine the degree of sequence similarity at the N-terminus. Amino acid sequences were aligned using the ClustalW algorithm and the BioEdit software.

ZMM molecular modeling

ZMM molecular modeling was used to determine binding affinities between the PB1 and PA subunits for various PB1 amino acid substitutions [15,16]. Energy calculations were performed in two stages. First, ZMM was used to generate a double-shell model around the PB1 peptide (residues 4-10) with a 12 Å flexible shell and a 15 Å rigid shell. This initial model was optimized by the Monte Carlo (MC) minimization method using the Amber force field for either 200,000 iterations or 10,000 no energy down minimization steps, whichever occurred first. Point mutants were then generated from this energy-minimized model, and a new double-shell model was produced with a 6 Å flexible shell and a 9 Å rigid shell surrounding the peptide. Each point mutant was then subjected to a second round of energy minimization using the same parameters as described previously. Relative values of free energy were calculated from n=4 independent rounds of MC-minimization performed using a randomly generated seed number.

Cloning

A construct consisting of the N-terminal 20 amino acids of the PB1 subunit ($PB1_{1-20}$) and the Tat nuclear localization signal (NLS) amino acid sequence (YGRKKRRQRRR) attached to His-MBP was made using overlapping PCR with primers containing flanking attB sequences for cloning with the Gateway System (Invitrogen™ Gateway™ recombination cloning, ThermoFisher Scientific, Burlington, Ontario). Gene fragments were first cloned into the p$DONOR_{201}$ entry vector and then cloned into the p*DESTHis-MBP* (vector #11805 in Addgene vector repository, Cambridge, MA) vector for recombinant protein expression. The C-terminus of the PA subunit of Influenza A/California/2009/H1N1 ($PA_{257-716}$) was amplified by PCR from the pCAGGS-ACal04PA vector (graciously donated to us by Dr. Toru Takimoto) and cloned using primers with flanking Gateway *attB* sites. The construct was then recloned into the desired expression plasmid. All constructs were confirmed by sequencing the p*DONR201* vectors at the MOBIX facility at McMaster University.

Recombinant protein expression and purification

Recombinant proteins were expressed in *E. coli* and purified by FPLC chromatography. Overnight cultures of *E. coli* BL21 (DE3) or Rosetta (DE3) pLysS cells containing expression plasmids were subcultured at a 1:50 ratio in 6L of LB broth supplemented with 100 µg/mL of ampicillin. Cells were incubated at 37°C with shaking at 250 RPM until the cultures reached an OD_{600} of 0.6 at which time they were induced with the addition of 0.5 mM IPTG. The cultures were then incubated at room temperature for an additional two hours, cells were collected by centrifugation at 8, 000 x g for 2 minutes at 4°C and resuspended in either Nickel A Buffer for 6xHis-tagged proteins (20 mM Tris-HCl pH 7.0, 0.03% LDAO, 0.02% β-mercaptoethanol, 500 mM KCl, 10% glycerol, 10 mM imidazole) or PBS for GST-tagged proteins. The cells were lysed by sonication, and centrifuged at 42, 000 x g for 45 minutes at 4°C to separate soluble proteins from the insoluble pellet. Recombinant proteins were purified by Fast Protein Liquid Chromatography (FPLC) using the Akta FPLC (GE Healthcare) and dialyzed into PBS containing 10% glycerol using the HiPrep 26/10 Desalting Column (GE Healthcare).

Virus inhibition assay

Madin-Darby Canine Kidney (MDCK) cells were seeded in shell vials at a concentration of 2.5 x 10^5 cells per vial MEM+10% FBS and incubated overnight at 37°C and 5% CO_2. Cells were infected

first, and then treated with peptide inhibitors or treated with peptide inhibitors then infected with virus. For pre-treatment cells were washed with sterile PBS and incubated with the recombinant peptide mimetic (His-MBP fusion constructs) in MEM medium without FBS for one hour at 37°C and 5% CO_2. The media was removed and the cells were infected with Influenza A (A/California/2009/H1N1) in MEM at an MOI of 0.1 using centrifugation assisted inoculation (1,500 rpm for 30 min) followed by incubation at 37o C for 30 minutes. The innoculum was then removed and the cells were treated with fresh peptide in MEM for 24 hours at 37°C and 5% CO_2. Alternatively, cells were infected first with virus then peptides were added to the medium at various times post infection (1-6 hr). Following a 24 hour incubation the monolayers were fixed with ice cold acetone for 30 minutes, washed and stained by immunofluorescent staining using the D-Ultra Respiratory Virus Screening DFA Reagent (Diagnostic Hybrids) for 30 minutes at room temperature and cells were visualized by fluorescence microscopy using the Olympus BX51 Fluorescence Microscope at 10X Magnification. The percent inhibition was calculated as (the number of infected cells/hpf in the absence of peptide minus the number of infected cells/hpf in the presence of peptide) divided by 100 x 100 percent.

Quantitative PCR

MDCK cells were seeded into 6 well plates and incubated at 37°C and 5% CO_2 until confluent. The cells were washed with 1 mL of sterile PBS and treated with 50 µM peptide mimetic in MEM for 1 hour at 37°C. The cells were then infected with pandemic H1N1 Influenza an in MEM (MOI = 0.1) for 2 hours at 37°C and 5% CO_2. The viral innoculum was removed and fresh medium containing 50 µM peptide (or PBS as control), was added and the plates were incubated at 37°C and 5% CO_2 for 24 hours. Cells were collected and total nucleic acid was extracted using the NucliSENS miniMAG extraction kit (Biomémireux, Laval QC) according to the manufacturer's guidelines. Viral transcript copy number was assessed using qRT-PCR for the matrix gene using the SuperScript ® III Platinum ® One-Step qRT-PCR kit (Invitrogen) according to the manufacturer's instructions. The number of copies per cell was calculated using β-actin qPCR to determine the cell number in the preparations. The decrease in viral copy number in the presence of peptide mimetics was calculated by comparing the copy number in the presence of peptide compared to the PBS control without peptide. The fold reduction in viral copy number was calculated by dividing the mean copy number/cell for the PBS control by the mean copy number/cell for the peptide. Inhibition experiments were performed in triplicate and the results expressed as mean +/- 2 SD.

Red blood cell lysis assay

Peptides were tested for cytotoxicity using a RBC lysis assay as described [17]. RBC lysis was assessed by spectrophotometry measuring the absorbance of cell supernatants at 420 nm. Purified RBCs ($5.0x10^8$ cells) from healthy donors were incubated with peptides at a final concentration of 50 µM in PBS at 37°C for various times from 1 to 72 hours. Sterile PBS and Lysis buffer (0.1% SDS, 1% Triton X-100) were used as negative and positive controls for cell lysis respectively. Following incubation at 37°C cells were collected by centrifugation at 1,000 x g for 5 minutes, the supernatants were transferred to wells of a 96 well clear-bottom plate and the absorbance was read at 420 nm using the Biotek MicroQuant Plate Reader. The percent lysis was calculated by substracting the A_{420nm} of the PBS control and comparing the net absorption to the positive lysis control. Experiments were performed in triplicate and the mean +/- 2SD calculated using an unpaired Student t-test.

MDCK toxicity assay

The effect of peptide mimetics on cell doubling times was assessed as described previously [18]. MDCK cells ($5.0x10^5$ cells/well in MEM+10%FBS) were seeded into wells of a 24-well plate were allowed to attach overnight. After 18 hr the media was removed and cells were incubated with peptide mimetics at 50 µM in MEM+10% FBS, MEM medium alone or 1% Triton X-100 (positive lysis control). After 0, 4, 8, 24, 48 and 72 hr the media was removed and the cells were washed with PBS, collected by trypsin treatment (5 µg/mL Trypsin-EDTA at 37°C for 10 minutes), transferred to a 1 cm cuvette. The absorbance was measured at 800 nm using 5 µg/mL Trypsin-EDTA buffers as blank. The A_{800nm} was plotted against time to determine the effect of peptides on cell doubling time.

Nuclear uptake of peptides

MDCK cells were incubated with 50 µM of peptide in MEM for 1 hour at 37°C. Cell monolayers were washed with PBS, treated with 0.5 mg/mL Trypsin to remove extracellular peptides, and then incubated for 10 min with cold nuclear extraction buffer (10 mM HEPES pH 7.9, 10 mM KCl, 0.1 mM EDTA, 0.4% IGEPAL, 1 mM DTT, 1 complete EDTA-free protease inhibitor). Cells were scraped with a cell scraper and lysates collected and centrifuged at 16, 000 x g for 3 minutes at 4°C to separate the nuclear and cytosolic fractions. Proteins were precipitated with 10% tetrachloroacetic acid (TCA) and collected by centrifugation at 16,000 x g for 20 minutes.

GST Pull down assay

E. coli lysates containing either GST-$PA_{257-716}$ or GST alone were incubated with Glutathione-agarose beads (Sigma-Aldrich, Oakville ON) for two hours at 4°C with shaking. After coupling proteins to the beads, the beads were collected by centrifugation, washed twice with PBS and incubated with 1 mg of purified recombinant His-MBP-NLS-$PB1_{1-20}$ or His-MBP-NLS as control overnight at 4°C. The beads were washed 4 times in a high salt buffer (20 mM Tris pH 7.0, 500 mM NaCl, 0.1% v/v Triton X-100). Aliquots of each wash were analysed by Western Blot using anti-His antibody.

Results

Interaction of PB1 and PA subunits

Influenza virus polymerase is a heterotrimeric complex made up of PA, PB1, and PB2 subunits. Biochemical and X-ray crystallographic studies have shown that the N-terminus of the PB1 subunit interacts with the C-terminus of PA [11,12]. In order to confirm

that the PB1 peptide could be taken up by cells and interact with polymerase subunits in the nucleus, we first constructed a fusion protein consisting of the PB1 peptide bound to Maltose Binding Protein (MBP) and the HIV Tat nuclear localization signal (NLS). His-MBP was chosen as the carrier molecule so it could be affinity purified on Ni columns and NLS was previously shown to facilitate translocation of proteins across the cytoplasmic membrane and into the cell nucleus [14,19]. We used an in vitro GST pull-down assay to confirm that recombinant PB1-MBP-NLS made in E. coli interacts with the PA subunit. Figure 1 shows that beads coated with GST-$PA_{257-716}$ pulled down His-MBP-NLS-$PB1_{1-20}$ protein while GST coated beads did not (Figure 1).

Figure 1

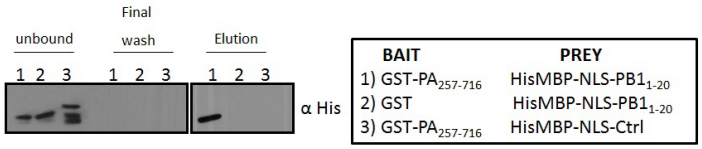

Figure 1: Interaction of HisMBP-NLS-$PB1_{1-20}$ GST-$PA_{257-716}$ peptides in vitro.

E. coli cell lysates containing recombinant GST-$PA_{257-716}$ or GST (bait) were first incubated with glutathione-agarose beads, washed and then incubated with either HisMBP-NLS-$PB1_{1-20}$ or a control peptide HisMBP-NLS-Ctrl (prey). The beads were washed, resuspended with 2X sample buffer and electrophoresed by SDS-PAGE. Unbound proteins, final wash and eluted proteins are shown. C-terminal GST tagged PA was able to pull down the HisMBP-NLS-$PB1_{1-20}$ peptide, while GST alone did not (elution fraction).

In silico molecular modeling of the $PB1_{1-20}$ and PA peptide interactions

Examination of the N-terminal 20 amino acids of the PB1 subunit of several different influenza a strains indicates that the first 20 amino acids are highly conserved (Figure 2A). We used ZMM molecular modeling of the published crystal structure of the PB1/PA complex (http://www.zmmsoft.com/) to investigate the binding avidity of the PB1-PA subunit interaction and to determine the hypothetical free energy of binding between PB1 and PA for different amino acids at different PB1 positions [15,16]. We identified two significant amino acid substitutions for threonine at position 6, viz. threonine to glutamic acid (T6E) and threonine to arginine (T6R) that had a lower free energy of binding (Figure 2B). Based on in silico modeling, we hypothesized that the $PB1_{1-20}$ peptides containing either T6E or T6R substitutions would have a higher binding affinity for the PA subunit and therefore have increased anti-influenza activity.

Figure 2

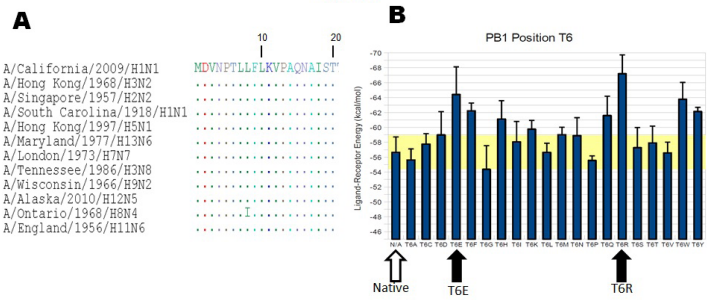

Figure 2: Conservation of the N-terminal amino acids of Influenza PB1 subunit and in silico ZMM molecular modeling of the $PB1_{1-20}$ interaction with PA. (A) The first 20 amino acids of PB1 from 12 different Influenza A strains were aligned using the ClustalW algorithm. Sequence identity is indicated with a dot compared to the top strain (pandemic 2009 H1N1 strain used in this study). (B) The crystal structure of C-terminal PA in complex with N-terminal PB1 was used to model different amino acid substitutions at various positions in the PB1 protein and calculate the hypothetical free energy of binding using ZMM analysis as described in Methods section. The in silico simulation yielded several lower energy state amino acids at position 6 viz. glutamic acid (T6E) and arginine (T6R) being highlighted (black arrows) compared to the wild type threonine (T) shown by the while arrow.

NLS transports peptides to the cell nucleus

The HIV Tat NLS peptide has been shown to be an effective cell penetrating peptide for directing peptides into the nuclear compartment [14]. We next wanted to confirm that the NLS peptide would deliver PB1-MBP into the nucleus of MDCK cells. His-MBP-NLS-PB1 was incubated with cells for 10 minutes and cell lysates were tested by Western blot analysis using anti-His antibody. Figure 3 shows that His-MBP-NLS-PB1 was taken up by cells while His-MBP or His-MBP-PB1 lacking the NLS sequence were not taken up by cells. The His-MBP-NLS-PB1 peptides containing a single amino acid substitution at position 6, either glutamic acid (T6E) or arginine (T6R), were also taken up by cells (Figure 3).

Figure 3

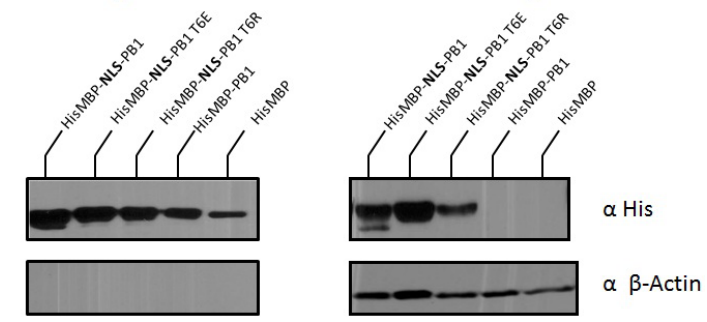

Figure 3: Uptake of MBP peptides containing a NLS peptide. MDCK cells were incubated for one hour with wild type peptide,His-MBP-NLS-PB1, or modified peptides, His-MBP-NLS-T6E or T6R, containing an NLS peptide or control His-MBP-PB1or His-MBP alone lacking an NLS. Cells were washed, treated with Trypsin, harvested and electropheresed by SDS-PAGE. Samples were blotted with antibodies against 6xHis and β-actin (loading control). Only proteins containing a nuclear localization signal were detected in MDCK cell lysates.

To confirm that the peptides are transported to the cell nucleus where polymerase-dependent transcription and genomic replication occur, cell nuclei were examined for the presence of peptides using Western blot analysis. MDCK cells were incubated with either His-MPB-NLS-$PB1_{1-20}$ peptides or His-MBP-$PB1_{1-20}$ lacking the NLS. Cells were then treated with a buffer containing IGEPAL/NP-40 detergent that solubilizes the plasma membrane but keeps the nuclear membrane intact and the cytosolic and nuclear fractions were tested by Western blotting with antibodies

directed against His_6, Actin (cytosolic protein), and Lamin A (inner nucleus protein). All three of the PB1 peptides containing NLS were present in the nuclear fraction (Figure 4). A control His-MBP-$PB1_{1-20}$ construct without an NLS was not detected in the nuclear or cytoplasmic fractions (Figure 4, lane 4). Only traces of NLS tagged proteins were detected in the cytoplasm, suggesting that NLS tagged proteins were efficiently translocated into the nucleus

Figure 4

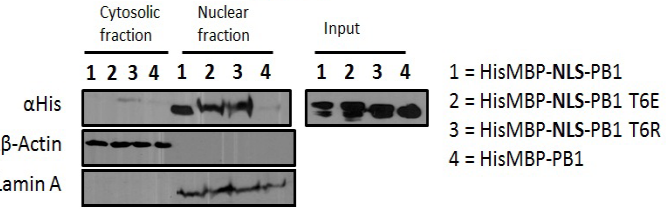

Figure 4: Transport of NLS-containing peptides into the cell nucleus. MDCK cells were incubated with His-tagged MBP proteins for one hour, cells were lysed 0.4% IGEPAL and nuclear and cytosolic fractions analyzed by western blot with anti-His, anti- β-actin (cytosolic protein) or Lamin A (nuclear protein) antibodies as described in the Methods section. All three MBP-PB1 proteins containing an NLS peptides (lanes 1,2 and 3) were detected in the nuclear fractions while MBP-PB1 lacking the NLS peptide was not present in the nucleus.

Increased potency of $PB1_{1-20}$ peptides with T6E and T6R

To investigate whether the T6E and T6R amino acid substitutions identified by ZMM analysis provide increased anti-viral activity we constructed recombinant proteins consisting of His-MBP with a NLS and $PB1_{1-20}$ containing either T6E or T6R (His-MBP-NLS-$PB1_{1-20}$ T6E/R). Recombinant proteins were incubated with MDCK cells for one hour and cells were infected with Influenza then stained at 24 hr for viral proteins by indirect immunofluorescence. The wild type PB1 peptide showed a dose dependent inhibition with 98% inhibition at 50 µM, 36% inhibition at 25 µM and 16% inhibition at 12.5 µM (Figure 5, panel a-c) while cells treated with 50 µM His-MBP-NLS lacking a PB1 peptides showed no inhibition (Figure 5A, panel k). All three peptides displayed dose-dependent responses, with 98% inhibition at 50 µM (Figure 5B). The T6E and T6R peptides showed greater inhibition than the wild type peptide (Figure 5B). At 25 µM, the wild type peptide showed 36% viral inhibition, compared to 71% for T6E and 77% for T6R peptide. At 12.5 µM, the wild type peptide showed 16% inhibition, while the T6E and T6R peptides displayed 27% and 70% inhibition, respectively. We next used qPCR to assess the effect of the three peptides on influenza virus transcription. Cells were treated with peptides then infected with influenza virus and matrix gene transcript levels were determined at 24 hours post infection. At a concentration of 25 µM the wild type PB1 peptide resulted in a 43.4-fold reduction in transcripts while the T6E and T6R peptides resulted in 70.1- and 136.3-fold reductions, respectively (Figure 5C) compared to controls without any peptide.

Lack of toxicity of peptide mimetics

We next wanted to confirm that these peptides did not have any adverse effect on cell integrity so the peptides were evaluated using a red blood cell lysis assay and an MDCK cell doubling assay. The red blood cell lysis assay involved incubating the peptides

Figure 5

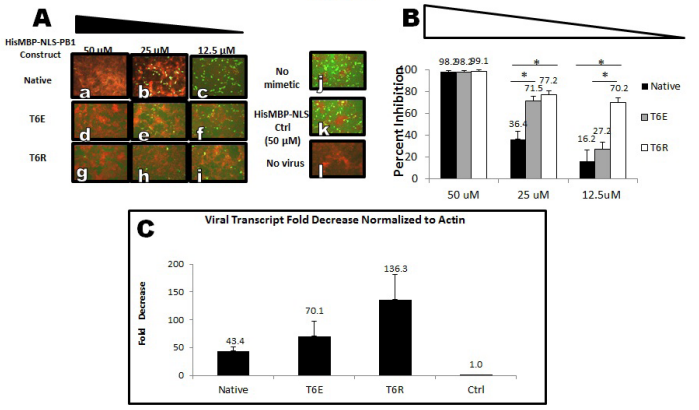

Figure 5: PB1 peptides with PB1 peptides with T6E or T6R substitutions have increased anti-Influenza activity. MDCK cells were incubated with MBP peptides containing either wild type PB1, T6E or T6R mutations for one hour and then infected with Influenza virus. (A) The number of virus infected cells per high power field were counted by indirect immunofluorescent staining. Influenza infected cells appear green and non-infected MDCK cells appear red. (B) Percent inhibition of wild type, T6E or T6R peptides from panel A. Black line= wild type PB1; grey line=T6E peptide; while line=T6R peptide. Data represents the mean of three independent experiments + 2 SD and * $p < 0.05$. (C) Reduction of influenza matrix gene transcripts by wild type and modified PB1 peptides. Cells were treated with three peptides, infected with influenza, and matrix gene transcripts quantified by qPCR as described in Methods section. The number of transcripts per cell was determined using normalization with beta-actin transcripts and the results were expressed as fold decrease for each peptide compared with no peptide controls.

with RBCs and measuring the release of hemoglobin that was measured by absorbance at 420 nm [17]. RBCs were incubated with the three peptides at 50 µM for 24, 48 and 72 hr and then lysis was assessed. There was no significant lysis with any of the three peptides at times up to 72 hr when compared to the PBS control. When compared to PBS alone all three peptides exhibited less than 7% lysis at all three time points, indicating that the peptides did not have any adverse effect on RBC membranes and lacked detectable toxicity (Figures 6A and 6B).

Figure 6

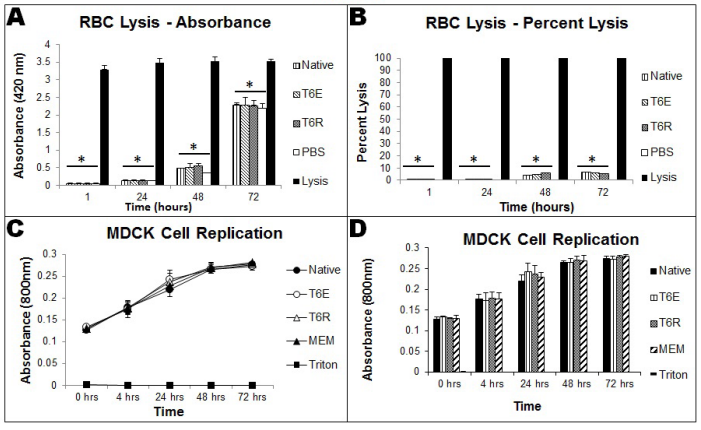

Figure 6: PB1 peptides do not lyse RBC or inhibit the replication of MDCK cells.

The toxicity of MBP-NLS-PB11-20 wild type, T6E and T6R peptides was assessed in vitro using a Red blood cell lysis assay (panel A and B) and

an MDCK cell doubling assay (panel C and D). (A) RBCs were incubated with PB1 peptides for 72 hr and cell lysis assessed by measuring the absorbance at 420 nm. A positive detergent lysis (black bar) treatment was included for comparison. The amount of lysis for all three PB1 peptides was similar to the PBS control. (B) The absorbance results for all three peptides in panel A are expressed as percent lysis and compared to the lysis control. The percent lysis for all three peptides were <5% and not significantly different from PBS (*p< 0.001). (C) MDCK cells were incubated for 72 hr in the presence or absence of PB1 mimetics and cell replication/doubling times determined by measuring the absorbance at 800 nm as described in Methods section; MEM medium alone without peptide, or Triton X-100 served as controls. (D) Absorbance results obtained in panel C were expressed as a bar graph to show the lack of effect of the peptides on cell replication. Error bars represent two standard deviations of the mean for triplicate readings.

We next examined whether the peptides had any effect on cell doubling times using an absorbance at 800_{nm} assay to assess cell numbers. MDCK cells were incubated with either wild type PB1, T6E, or T6R peptides, media alone, or media containing Triton X-100 detergent for 72 hours as described in the Methods section. Cells were harvested at various time points, then lysed and the absorbance at 800 nm measured to assess cell number. At 24, 48 and 72 hours the absorbance for cells treated with all three peptides was the same as that of the PBS control indicating that the peptides had no effect on cell doubling times (Figures 6C and 6D). The results for the MDCK cell doubling are consistent with those obtained for the RBC lysis assay indicating that the PB1 peptides were non-toxic to cells.

Discussion

Influenza continues to represent a major infectious disease burden globally with infections resulting to loss of economic output, increased hospitalizations and deaths. While vaccines can be an effective strategy in controlling infection, they require annual updates since influenza mutates continually making vaccines less effective as new viruses become resistant to host neutralizing antibodies and therapeutic anti-virals [3,20]. Although antivirals have been shown to be effective against Influenza, resistance to these drugs is increasing and newer therapeutics is required. The conserved interacting domains of the RNA polymerase represent novel therapeutic targets for peptide mimetics [3,7,21,22]. We show here that a peptide mimetic containing the N-terminal portion of PB1 can be attached to carrier protein containing a cell penetration peptide and delivered to cells to prevent virus replication. We show also that in silico ZMM molecular modeling could be used to develop a peptide mimetic with increased antiviral activity.

Based on the known interaction between the N-terminus of PB1 and the C-terminus of PA subunits, Ghanem et al. [13] showed that a $PB1_{1-25}$ peptide acting as a peptide mimetic reduced influenza viral titers in plasmid-transformed HEK293 cells following influenza infection. These authors' transformed HEK293 cells with a plasmid that could synthesize the $PB1_{1-25}$ peptide and showed that it inhibited influenza virus replication. We have extended the work of these authors by showing that a PB1 peptide attached to a carrier protein and a cell penetration peptide (NLS) can be delivered to cells and inhibit virus transcription and translation. We used the HIV Tat_{47-57} NLS to deliver the peptide to the nucleus where the influenza RNA polymerase carries out both transcription and genomic replication. When added to MDCK cells that were subsequently infected with influenza, the peptide mimetics inhibited virus replication by 98% in a dose-dependent fashion (Figure 5B).

We next used *in silico* ZMM molecular modeling in an attempt to develop a peptide with increased antiviral activity. Molecular modeling predicted that two amino acid substitutions at position 6 should result in peptides with increase in binding affinity and we showed that two modified peptides T6E and T6R had increased levels of antiviral activity compared to the wild type peptide (Figure 5). The T6R peptide appeared to be the more effective of the two, as it exhibited 70% inhibition at 12.5 µM, whereas the wild type peptide and T6E exhibited a 16.2% and 27.2% inhibition respectively. We next used qPCR to measure the level of viral transcripts and showed that both T6E and T6R peptides were more effective at decreasing transcription compared with the wild type peptide; matrix gene transcripts were decreased 70- and 136-fold with T6E and T6R respectively compared with 43-fold reduction for the wild type peptide (Figure 5C). The increased activity of T6E and T6R for decreasing transcription and protein synthesis was consistent with the ZMM molecular modeling prediction that these peptides would have greater affinity and anti-viral activity compared to the native peptide.

Our results for the T6E and T6R peptides differ somewhat from work published by Wunderlich et al. (2009) who used a competitive ELISA screening assay to assess PB1-PA interactions [23]. They showed that a tyrosine, phenylalanine, or cysteine substitution at position 6 rendered PB1 peptides with increased potency as assessed by a plaque reduction assay. The screen performed by these authors did not identify arginine or glutamic acid substitutions giving PB1 peptides increased antiviral activity. The crystal structure of PB1N-PAC complex suggests that a lack of contact between threonine at position 6 and PA could be exploited by amino acid substitutions to create an interaction with the nearby Leu 666 and/or Phe 710 residues of PA [12]. The relatively bulky and charged glutamic acid and arginine amino acids most likely fit inside the binding pocket of PA better than the smaller threonine residue and is predicted to form hydrogen bonds with either the amine or carbonyl group of the polypeptide backbone. One would also expect hydrophobic interactions between side chain groups of Leu 666/Phe 710 with a hydrophobic amino acid such as phenylalanine as suggested by these authors [24] and our ZMM modeling (Figure 2B). These amino acid interactions could explain the increased antiviral activity seen with the T6E and T6R peptides.

Wunderlich et al. (2011) recently used a structure-affinity relationship analysis and showed that all of the amino acids in the core binding region of PB1 (aa 5-11) are indispensable for PA binding. Using a library of immobilized peptides they were able to show that 5 amino positions (aa 1,3,12,14,15) outside the

core binding region can be replaced by affinity-enhancing residues [24]. When re-tested by the competitive ELISA, only 2 of 11 peptides showed increased IC50s and all the remaining peptides had IC50 values lower than the native PB1 which suggests that biochemical interaction assays do not accurately reflect antiviral activity levels. For this reason, peptide amino acid substitutions should be evaluated for their ability to inhibit virus replication using either a plaque reduction assay or IF staining.

Molecules with a molecular weight over 900 Daltons cannot passively diffuse through the plasma membrane, and therefore require the addition of a cell-penetrating peptide (CPP) to transport them through the cytoplasmic membrane. Other groups have shown that the HIV Tat NLS is sufficient to transport large proteins (such as the ~40 kDa Maltose Binding Protein) through the plasma membrane and into the cytoplasm [25]. We designed our PB1 peptides with a NLS to target them to the nucleus where they would interact with the PA subunit thereby preventing assembly of an active polymerase complex. Using nuclear purification and Western blot analysis with anti-lamin A antibody to stain the inner nuclear membrane [26] we showed that the cell penetrating peptide NLS successfully transported the peptides into the nucleus where they inhibited transcription and cytoplasmic protein synthesis as assessed by IF staining. We also showed that these peptide mimetics were not toxic to cells as they did not cause hemolysis of red blood cells an established indicator of cytotoxicity [17] not did they affect the doubling times of MDCK cells as determined by measuring the absorbance at 800 nm [18]. These PB1 peptide mimetics represent a novel class of therapeutic which if proven efficacious in animal models could augment our limited number of antivirals for treating influenza infections.

Acknowledgements

We gratefully acknowledge the secretarial assistance of Joanne Warner.

References

1. Molinari NA, Ortega-Sanchez IR, Messonnier ML. et al. The annual impact of seasonal influenza in the US: measuring disease burden and costs. Vaccine. 2007; 27: 5086-5096.
2. Hurt AC. The epidemiology and spread of drug resistant human influenza viruses. Curr Opin Virol. 2014; 8: 22-29.
3. Cheng VC, To KK, Tse H, et al. Two Years after Pandemic Influenza A/2009/H1N1: What Have We Learned? Clin Microbiol Rev. 2012; 25: 223-263.
4. Das K, Aramini JM, Ma LC, et al. Structures of influenza A proteins and insights into antiviral drug targets. Nat Struct Mol Biol. 2010; 17: 530-538.
5. Bright RA, Shay DK, Shu B, et al. Adamantane resistance among influenza A viruses isolated early during the 2005-2006 influenza season in the United States. JAMA. 2006; 295: 8-11.
6. World Health Organization. Review of the 2010-2011 winter influenza season, northern hemisphere. Wkly Epidemiol Rec. 2011; 86: 222–227.
7. Tsai CH, Lee PY, Stollar V, et al. Antiviral therapy targeting viral polymerase. Curr Pharm Des. 2006; 11: 1339-1355.
8. Gonzalez S, Zurcher T, Ortín J. Identification of two separate domains in the influenza virus PB1 protein involved in the interaction with the PB2 and PA subunits: a model for the viral RNA polymerase structure. Nucleic Acids Res. 1996; 15: 4456-4463.
9. Toyoda T, Adyshev DM, Kobayashi M. Molecular assembly of the influenza virus RNA polymerase: determination of the subunit-subunit contact sites. J Gen Virol. 1996; 77: 2149-2157.
10. ElHefnawi M, Alaidi O, Mohamed N. et al. (2011) Identification of novel conserved functional motifs across most Influenza A viral strains. Virol J 8: 44-51.
11. He X, Zhou J, Bartlam M. et al. (2008) Crystal structure of the polymerase PA(C)-PB1(N) complex from an avian influenza H5N1 virus. Nature 454: 1123-1126.
12. Obayashi E, Yoshida H, Kawai F. et al. (2008) The structural basis for an essential subunit interaction in influenza virus RNA polymerase. Nature 454: 1127-1131.
13. Ghanem A, Mayer D, Chase G. et al. (2007) Peptide-mediated interference with influenza A virus polymerase. J virol 14: 7801-7804.
14. Efthymiadis A, Briggs LJ, Jans DA. (1998) The HIV-1 Tat nuclear localization sequence confers novel nuclear import properties. J Biol Chem 273: 1623-1628.
15. Zhorov BS, Bregestovski PD. Modeling chloride channels of glycine and GABA receptors with blockers. Biophys J. 2000; 78: A2092.
16. Blanchet J, Lin SX, Zhorov BS. Mapping of steroids binding to 17 beta-hydroxysteroid dehydrogenase type 1 using Monte Carlo energy minimization reveals alternative binding modes. Biochemistry. 2005; 44: 7218–7227.
17. Blocker A, Gounon P, Larquet E. et al. (1999) The tripartite type III secreton of Shigella flexneri inserts IpaB and IpaC into host membranes. J Cell Biol 147: 683-693.
18. Mohler WA, Charlton CA, Blau HM. (1996) Spectrophotometric quantitation of tissue culture cell number in any medium. Biotechniques 21: 264-266.
19. Nallamsetty S, Austin BP, Penrose KJ, Waugh DS. (2005) Gateway vectors for the production of combinatorially-tagged His6-MBP fusion proteins in the cytoplasm and periplasm of Escherichia coli. Protein Sci 12: 2964-2971.
20. Drake JW. (1993) Rates of spontaneous mutation among RNA viruses. Proc Natl Acad Sci U S A 90: 4171-4175.
21. Guu TS, Dong L, Wittung-Stafshede P, Tao YJ. (2008) Mapping the domain structure of the influenza A virus polymerase acidic protein (PA) and its interaction with the basic protein 1 (PB1) subunit. Virology 379: 135-142.
22. von Itzstein M. (2007) The war against influenza: discovery and development of sialidase inhibitors. Nat Rev Drug Discov 12: 967-974.
23. Wunderlich K, Mayer D, Ranadheera C. et al. (2009) Identification of a PA-binding peptide with inhibitory activity against influenza A and B virus replication. PLoS One 10: e7517.
24. Wunderlich K, Juozapaitis M, Ranadheera C. et al. (2011).

Identification of high-affinity PB1-derived peptides with enhanced affinity to the PA protein of influenza A virus polymerase. Antimicrob Agents Chemother 55: 696-702.

25. Tunnemann G, Martin RM, Haupt S, Patsch C, Edenhofer F, Cardoso MC. (2006) Cargo-dependent mode of uptake and bioavailability of TAT-containing proteins and peptides in living cells. FASEB J 11: 1775-1784.
26. Dechat T, Pfleghaar K, Sengupta K. et al. (2008) Nuclear lamins: major factors in the structural organization and function of the nucleus and chromatin. Genes Dev 22: 832-853.